Molecular Therapy
Oncolytics
Original Article

RUNX1/EGFR pathway contributes to STAT3 activation and tumor growth caused by hyperactivated mTORC1

Wei Lin,[1,2,6] Xiaofeng Wan,[2,3,6] Anjiang Sun,[2,6] Meng Zhou,[2] Xu Chen,[2] Yanling Li,[2] Zixi Wang,[2] Hailiang Huang,[2] Hongwu Li,[4] Xianguo Chen,[5] Juan Hua,[2] and Xiaojun Zha[2]

[1]Department of Stomatology, The First Affiliated Hospital of Anhui Medical University, Hefei 230031, China; [2]Department of Biochemistry & Molecular Biology, School of Basic Medicine, Anhui Medical University, Hefei 230031, China; [3]Department of Laboratory, Cancer Hospital, Chinese Academy of Sciences, Hefei 230031, China; [4]Department of Otorhinolaryngology, Head & Neck Surgery, The Fourth Affiliated Hospital of Anhui Medical University, Hefei 230031, China; [5]Department of Urology, The First Affiliated Hospital of Anhui Medical University, Hefei 230031, China

Loss of function of tuberous sclerosis complex 1 or 2 (TSC1 or TSC2) leads to the activation of mammalian target of rapamycin complex 1 (mTORC1). Hyperactivated mTORC1 plays a critical role in tumor growth, but the underlying mechanism is still not completely elucidated. Here, by analyzing Tsc1- or Tsc2-null mouse embryonic fibroblasts, rat Tsc2-null ELT3 cells, and human cancer cells, we present evidence for the involvement of epidermal growth factor receptor (EGFR) as a downstream target of mTORC1 in tumor growth. We show that mTORC1 leads to increased EGFR expression through up-regulation of runt-related transcriptional factor 1 (RUNX1). Knockdown of EGFR impairs proliferation and tumoral growth of Tsc-deficient cells, while overexpression of EGFR promotes the proliferation of the control cells. Moreover, the mTOR signaling pathway has been shown to be positively correlated with EGFR in human cancers. In addition, we demonstrated that EGFR enhances cell growth through activation of signal transducer and activator of transcription 3 (STAT3). We conclude that activation of the RUNX1/EGFR/STAT3 signaling pathway contributes to tumorigenesis caused by hyperactivated mTORC1 and should be targeted for the treatment of mTORC1-related tumors, particularly TSC.

INTRODUCTION

The highly conserved serine/threonine protein kinase mammalian target of rapamycin (mTOR) plays a critical role in a battery of cellular processes, including cell growth, metabolism, autophagy, and ferroptosis, by integrating multiple extracellular and intracellular cues.[1,2] mTOR organizes itself into two functional multiprotein complexes, mTOR complex 1 (mTORC1) and mTOR complex 2 (mTORC2).[1] mTORC1 is composed of mTOR, Raptor, mLST8, PRAS40, and Deptor, whereas mTORC2 consists of mTOR, Rictor, and several other binding proteins.[1] Rapamycin is an acute inhibitor of mTORC1, whereas mTORC2 is relatively insensitive to rapamycin.[1] mTORC1 is frequently activated in human cancers, owing to gain-of-function mutations of proto-oncogenes, such as phosphatidylinositol 3-kinase (PI3K) and AKR mouse T cell lymphoma oncoprotein (AKT), or loss-of-function mutations of tumor suppressors, such as phosphatase and tensin homolog deleted from chromosome 10 (PTEN) and tuberous sclerosis complex 1 or 2 (TSC1 or TSC2).[3] TSC2 is a guanosine triphosphatase (GTPase)-activating (GAP) protein that binds to TSC1, forming a complex that negatively regulates a small GTPase, Ras homolog enriched in brain (Rheb).[4] AKT can phosphorylate and inactivate TSC2, which destabilizes TSC2 and disrupts its interaction with TSC1.[5,6] Disruption of the TSC1-TSC2 complex results in the accumulation of GTP-bound Rheb, which in turn stimulates mTORC1 kinase activity.[7] Hyperactivated mTORC1 phosphorylates its downstream targets p70S6K and 4EBP1, leading to accelerated protein synthesis, cell proliferation, and tumor growth,[1] but the underlying mechanisms remain unclear.

Epidermal growth factor receptor (EGFR), a member of the ErbB receptor tyrosine kinases family, plays a crucial role in growth, differentiation, and motility of cells.[8] Ligands such as EGF, binding to the extracellular domain of EGFR, lead to receptor dimerization and activation, causing the activation of several signal transduction cascades, mainly the AKT, MAPK, and JNK pathways.[8] Overexpression of EGFR has been described in a wide variety of tumors and is mostly associated with poor prognosis.[9] Currently, two classes of EGFR inhibitors have been developed and used for the treatment of some cancers, including small-molecule tyrosine kinase inhibitors such as gefitinib and monoclonal antibodies such as cetuximab.[9] However, the transcriptional regulation and the function of EGFR in mTORC1-related tumors remain largely unknown.

Received 18 April 2021; accepted 26 October 2021;
https://doi.org/10.1016/j.omto.2021.10.009.

[6]These authors contributed equally

Correspondence: Juan Hua, Department of Biochemistry & Molecular Biology, School of Basic Medicine, Anhui Medical University, Hefei, China.
E-mail: hjhuajuan@163.com
Correspondence: Xiaojun Zha, Department of Biochemistry & Molecular Biology, School of Basic Medicine, Anhui Medical University, Hefei, China.
E-mail: zhaxiaojunpumc@gmail.com

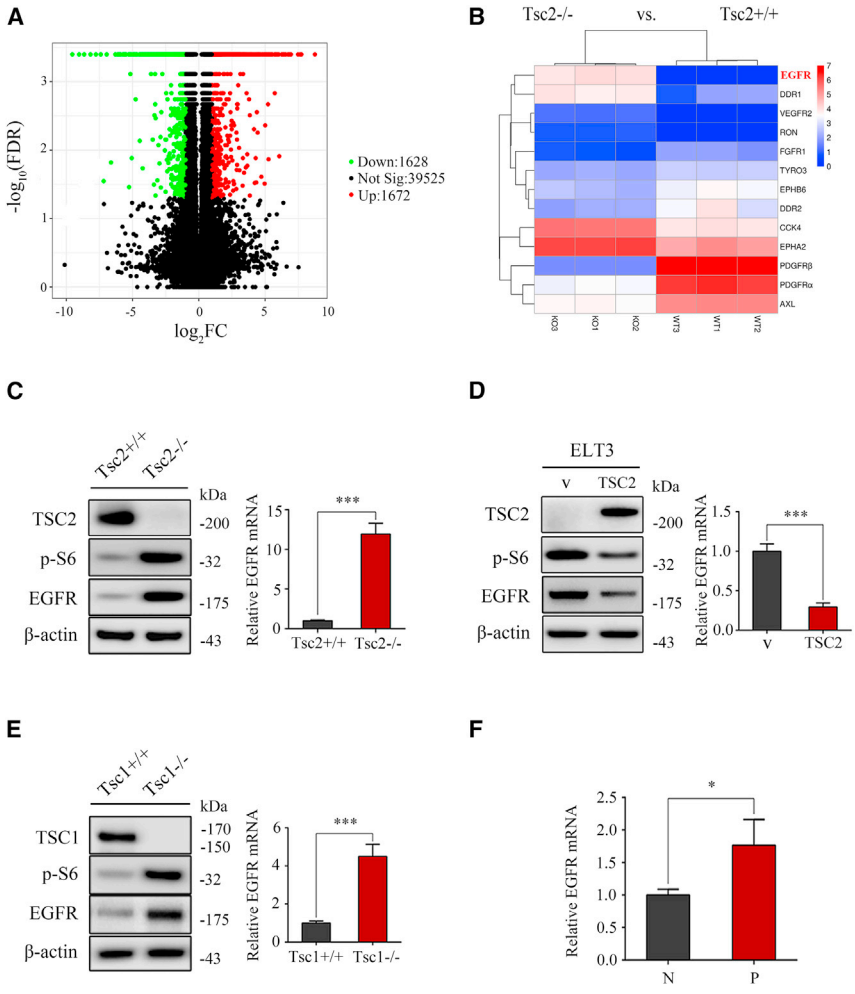

Figure 1. Loss of TSC1 or TSC2 upregulates the expression of EGFR

(A) A volcano plot shows the statistically upregulated (red) and downregulated (green) genes between Tsc2$^{-/-}$ and Tsc2$^{+/+}$ MEFs. (B) Heatmap exhibits the common cell membrane receptor genes between Tsc2$^{-/-}$ and Tsc2$^{+/+}$ MEFs. (C) Tsc2$^{+/+}$ and Tsc2$^{-/-}$ MEFs. (D) ELT3 cells were transduced with the retroviruses for human TSC2 (hTSC2) in pLXIN or its control vector pLXIN (V). (E) Tsc1$^{+/+}$ and Tsc1$^{-/-}$ MEFs. In (C) to (E), cell lysates were subjected to immunoblotting with the indicated antibodies (left panels). EGFR mRNA was analyzed by qRT-PCR (right panels). (F) Analysis of the mRNA abundance of EGFR in tissues from TSC patients by using mRNA microarray data from the GEO database (GEO: GSE9715). N, normal skin; A, facial angiofibromas; P, periungual fibromas. (n = 3). Error bars indicate mean ± SD of triplicate samples. *p < 0.05, ***p < 0.001.

In the present study, based on the analysis of Tsc1-null or Tsc2-null mouse embryonic fibroblasts (MEFs), rat uterine leiomyoma-derived Tsc2-null ELT3 cells, and human cancer cells, we demonstrate that mTORC1 positively regulates the expression of EGFR through upregulation of runt-related transcriptional factor 1 (RUNX1). Upregulated EGFR promotes the proliferation of cells with hyperactivated mTORC1 through activation of signal transducer and activator of transcription 3 (STAT3). Our findings provide a novel molecular mechanism for the tumorigenesis driven by dysregulated mTORC1 signaling, suggesting that components of the RUNX1/EGFR/STAT3 pathway may be potential targets for the treatment of TSC and some mTORC1-related tumors.

RESULTS

Loss of TSC1 or TSC2 upregulates the expression of EGFR

Receptor tyrosine kinases (RTKs) play an important role in tumor growth.[10] Platelet-derived growth factor receptor α (PDGFRα) and PDGFRβ have been found to be dysregulated as a result of loss of function of the TSC1-TSC2 complex.[11,12] To investigate whether the expression of other RTKs was changed upon loss of TSC2, RNA sequencing (RNA-seq) was performed to analyze differences in gene expression profiles between Tsc2$^{+/+}$ and Tsc2$^{-/-}$ MEFs. When compared with that of Tsc2$^{+/+}$ MEFs, RNA-seq analysis revealed a total of 3,300 differentially expressed genes (1,672 upregulated genes and 1,628 downregulated genes) in Tsc2$^{-/-}$ MEFs (Figure 1A). Consistent with previous reports,[11,12] PDGFRα and PDGFRβ expression significantly decreased in Tsc2$^{-/-}$ MEFs as compared with the control cells (Figure 1B). Interestingly, among the 13 differentially expressed RTK genes between Tsc2$^{-/-}$ and Tsc2$^{+/+}$ MEFs (log_2 fold change >1, $p < 0.05$), EGFR with the most significant change in expression (fold change = 14.9) was dramatically elevated upon loss of TSC2 (Figure 1B). Western blot and quantitative real-time PCR (qRT-PCR) analyses confirmed that EGFR expression markedly increased in Tsc2$^{-/-}$ MEFs (Figure 1C). Furthermore, ectopic expression of wild-type human TSC2 (hTSC2) abated the expression of EGFR in rat uterine leiomyoma-derived Tsc2-null ELT3 cells (Figure 1D). Because TSC1 stabilizes TSC2 as a binding partner,[6] we also evaluated the expression of EGFR in Tsc1$^{-/-}$ MEFs and Tsc1$^{+/+}$ MEFs. As expected, EGFR expression substantially increased in Tsc1$^{-/-}$ MEFs compared with the control cells (Figure 1E). In addition, a search using the Gene Expression Omnibus (GEO) database (accession number GEO: GSE9715) revealed that EGFR transcript levels increased in periungual fibroma tissues (typical skin lesions in TSC patients) in comparison with normal skin tissues (Figure 1F). Taken together, the results show that loss of TSC1 or TSC2 upregulates the expression of EGFR.

Loss of TSC1 or TSC2 increases EGFR expression via activation of mTORC1

The predominant and central event in TSC1 or TSC2 deficiency is constitutive activation of mTORC1.[4] Because loss of TSC1/TSC2

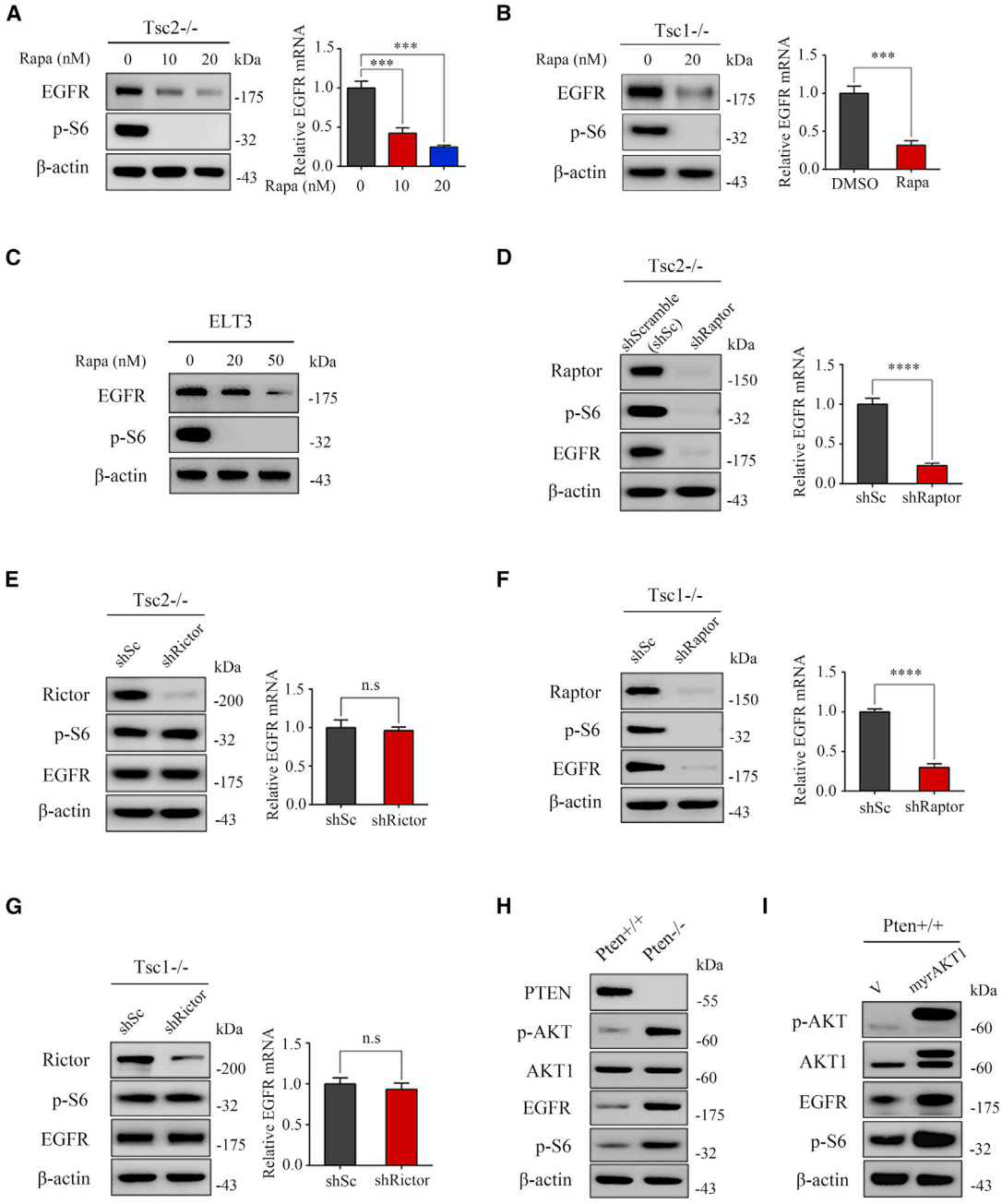

Figure 2. mTOR is a positive regulator of EGFR

(A–C) Tsc2$^{-/-}$ MEFs (A), Tsc1$^{-/-}$ MEFs (B), or ELT3 cells (C) were treated with DMSO or rapamycin for 24 h. (D and F) Tsc2$^{-/-}$ (D) or Tsc1$^{-/-}$ (F) MEFs were transduced with shRaptor or shScramble (shSc) lentiviruses. (E and G) The shRNA that silences Rictor (shRictor) or a control shRNA (shSc) were stably expressed in Tsc2$^{-/-}$ MEFs (E) or Tsc1$^{-/-}$ MEFs (G). (H) Pten$^{+/+}$ and Pten$^{-/-}$ MEFs. (I) Pten$^{+/+}$ MEFs transduced with the retroviruses for myristoylated AKT1 (myrAKT1) in pLXIN or its control vector pLXIN (V). In (A), (B), and (D) to (G), cell lysates were subjected to immunoblotting with the indicated antibodies (left panels). qRT-PCR was performed to detect the mRNA level of EGFR (right panels). In (C), (H), and (I), cell lysates were subjected to immunoblotting. Error bars indicate mean ± SD of triplicate samples. ***$p < 0.001$, ****$p < 0.0001$; n.s indicates no significant difference.

complex eventually leads to hyperactivation of mTORC1 (p-S6 is an indicator of mTORC1 activity) and the concomitant upregulation of EGFR, we hypothesized that mTORC1 participates in the regulation of EGFR upon loss of TSC1 or TSC2. To test this hypothesis, we first evaluated the effect of rapamycin, a specific mTORC1 inhibitor, on EGFR expression in Tsc2$^{-/-}$ MEFs. As shown in Figure 2A,

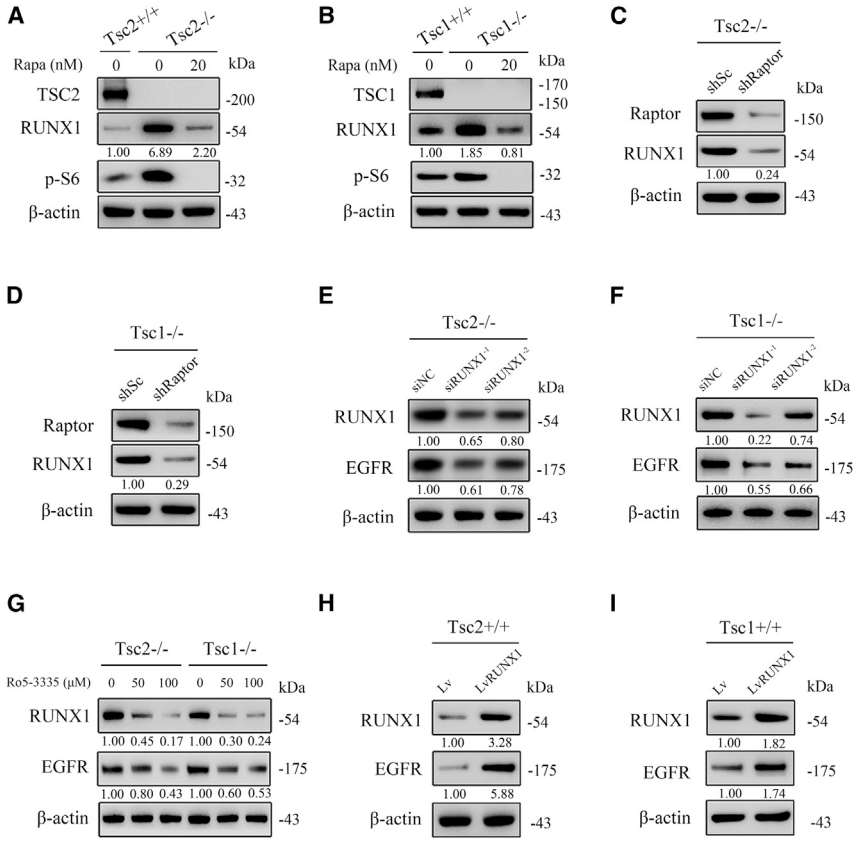

Figure 3. mTORC1 promotes the expression of EGFR by upregulating RUNX1

(A) Tsc2$^{+/+}$ MEFs, Tsc2$^{-/-}$ MEFs, and rapamycin (20 nM, 24 h) treated Tsc2$^{-/-}$ MEFs. (B) Tsc1$^{+/+}$ MEFs, Tsc1$^{-/-}$ MEFs, and rapamycin (20 nM, 24 h) treated Tsc1$^{-/-}$ MEFs. (C and D) Tsc2$^{-/-}$ MEFs (C) or Tsc1$^{-/-}$ MEFs (D) were infected with lentiviruses harboring vectors encoding Raptor shRNA (shRaptor) or the control shRNA (shSc). (E and F) Tsc2$^{-/-}$ (E) or Tsc1$^{-/-}$ (F) MEFs were transfected with control siRNAs (siNC) or siRNAs against RUNX1 for 48 h. (G) Tsc2$^{-/-}$ or Tsc1$^{-/-}$ MEFs were treated with or without Ro5-3335 (50 or 100 μM) for 24 h. (H and I) Tsc2$^{+/+}$ (H) or Tsc1$^{+/+}$ (I) MEFs were transduced with the lentiviruses for RUNX1 in GV367 or its control vector GV367 (LV). In (A) to (I), cell lysates were subjected to western blot analysis using the indicated antibodies. The intensities of protein bands were quantified using ImageJ software and normalized by the amounts of β-actin; relative amounts are shown below each lane.

inhibition of mTORC1 led to a marked reduction of EGFR expression at both protein and mRNA levels. Similarly, EGFR levels dramatically decreased in Tsc1$^{-/-}$ MEFs and ELT3 cells in response to rapamycin treatment (Figures 2B and 2C).

mTOR exists in two multiprotein complexes, rapamycin-sensitive mTORC1 and rapamycin-insensitive mTORC2.[1] To further verify that mTORC1 positively regulates EGFR, we examined the expression level of EGFR in Raptor (a specific component of mTORC1) or Rictor (a specific component of mTORC2) knockdown Tsc2$^{-/-}$ MEFs. As shown in Figures 2D and 2E, cells transfected with Raptor short hairpin RNAs (shRNAs) exhibited decreased EGFR levels, while Rictor shRNAs had little effect on the expression of EGFR. Furthermore, depletion of Raptor or Rictor in Tsc1$^{-/-}$ MEFs led to results similar to those in Tsc2$^{-/-}$ MEFs (Figures 2F and 2G).

In addition to genetic loss of TSC1 or TSC2, mTORC1 can also be activated by the inactivation of the tumor suppressor PTEN or the overexpression of a myristoylated AKT1 (myrAKT1).[13] As expected, cells with either deletion of PTEN or ectopic expression of myrAKT1 displayed a remarkable increase in expression of EGFR (Figures 2H and 2I). Taken together, the results show that hyperactivated mTORC1 signaling is responsible for the upregulation of EGFR.

mTORC1 upregulates EGFR through upregulation of RUNX1

The RUNX family transcription factors, including RUNX1, RUNX2, and RUNX3, plays an essential role in diverse functions in mammalian cells and modulates the transcription of its target genes by recognizing the core consensus DNA-binding sequences, namely, the classic 5′-TGTGGT-3′ motif.[14,15] It has been suggested that EGFR is a downstream target of RUNX2 in melanoma cells.[16] Interestingly, by analyzing our RNA-seq data, we found that among the three RUNX genes, only RUNX1 showed a substantial increase in mRNA levels in Tsc2-null MEFs compared with the control cells (Table S1). Furthermore, analysis using the GEPIA dataset indicated that RUNX1 has a positive correlation with EGFR in multiple cancers (Figure S1). Taken together, these findings prompted us to investigate the potential role of RUNX1 in mTORC1-mediated upregulation of EGFR.

Next, we evaluated the protein expression of RUNX1 in Tsc2$^{-/-}$ MEFs and the control cells. As shown in Figure 3A, RUNX1 was significantly upregulated in Tsc2-null MEFs and was normalized in response to rapamycin treatment. Similarly, loss of TSC1 also led to the upregulation of RUNX1, and its expression was markedly decreased with mTORC1 inhibition (Figure 3B). We also investigated whether the expression of RUNX1 is controlled by mTORC1 by using lentiviral vectors expressing shRNAs targeting Raptor in Tsc2$^{-/-}$ or Tsc1$^{-/-}$ MEFs. As shown in Figures 3C and 3D, knocking down Raptor led to the downregulated expression of RUNX1 in both Tsc2$^{-/-}$ and Tsc1$^{-/-}$ MEFs. It thus appears that hyperactivated mTORC1 signaling is responsible for the upregulation of RUNX1.

Activation of mTORC1 led to both upregulation of RUNX1 and EGFR expression, so we next investigated whether mTORC1 upregulation of EGFR is mediated by RUNX1. As depicted in Figures 3E and

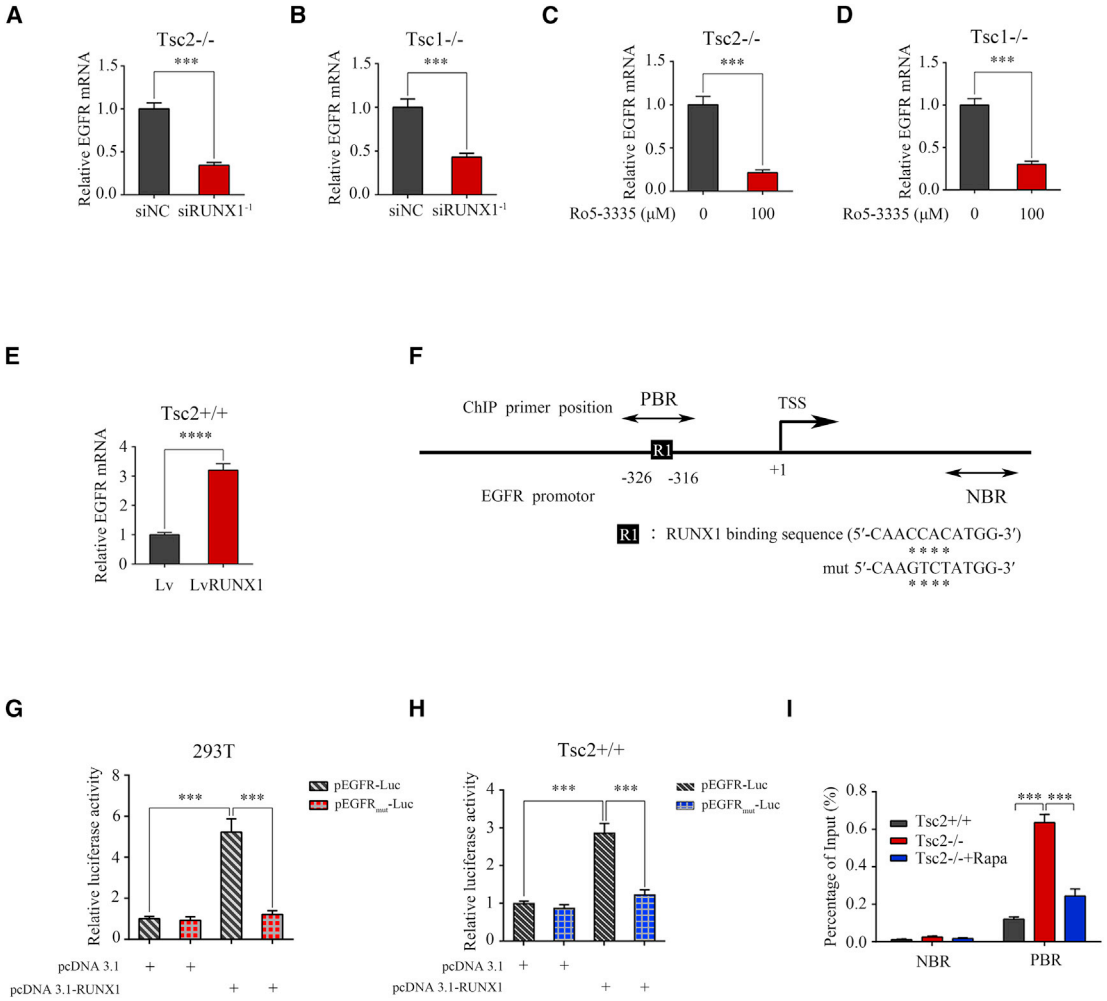

Figure 4. RUNX1 directly transactivates EGFR expression

(A and B) Tsc2$^{-/-}$ MEFs (A) or Tsc1$^{-/-}$ MEFs (B) were transfected with siRNAs targeting RUNX1 or the control siRNAs (siNC) for 48 h. (C and D) Tsc2$^{-/-}$ MEFs (C) or Tsc1$^{-/-}$ MEFs (D) were treated with or without Ro5-3335 for 24 h. (E) Tsc2$^{+/+}$ MEFs were transduced with Lv-RUNX1 or Lv lentiviruses. In (A) to (E), the mRNA level of EGFR of the indicated cells was analyzed by qRT-PCR. (F) Schematic representation of the putative RUNX1-binding site in the promoter of mouse EGFR gene. (G and H) HEK 293T cells (G) or Tsc2$^{+/+}$ MEFs (H) were co-transfected with pEGFR-Luc or pEGFR$_{mut}$-Luc plus pcDNA 3.1-RUNX1 or control pcDNA 3.1 and the internal control plasmid pRL-TK. Relative luciferase activity was detected 24 h after transfection. (I) Tsc2$^{+/+}$, Tsc2$^{-/-}$, and rapamycin-treated Tsc2$^{-/-}$ MEFs were subjected to a ChIP analysis of RUNX1-binding site in EGFR promoter region using an anti-RUNX1 antibody. Normal rabbit IgG antibody served as negative control. qRT-PCR was performed to amplify regions surrounding the putative RUNX1-binding region (PBR) and a nonspecific RUNX1-binding region (NBR). The data were plotted as the ratio of immunoprecipitated DNA subtracting nonspecific binding to IgG versus total input DNA (%). Representative data from three independent experiments are shown. Data indicate mean ± SD of triplicate samples. ***$p < 0.001$, ****$p < 0.0001$.

3F, knocking down RUNX1 in Tsc2$^{-/-}$ or Tsc1$^{-/-}$ MEFs markedly reduced RUNX1 and EGFR expression. Pharmacologic inhibition of RUNX1 by a small-molecule inhibitor, Ro5-3335, also led to the downregulated expression of EGFR in both Tsc2-null and Tsc1-null MEFs (Figure 3G). In addition, Tsc2$^{+/+}$ or Tsc1$^{+/+}$ MEFs were also transfected with lentiviruses overexpressing RUNX1. Ectopic expression of RUNX1 significantly promoted the expression of EGFR (Figures 3H and 3I). Collectively, the results show that mTORC1 promotes the expression of EGFR via upregulation of RUNX1 in Tsc1- or Tsc2-null MEFs.

EGFR expression is directly transactivated by RUNX1

To clarify the molecular mechanisms underlying the regulation of EGFR by RUNX1, we extracted total RNAs from RUNX1 small interfering RNA (siRNA)-transfected Tsc2$^{-/-}$ or Tsc1$^{-/-}$ MEFs and their corresponding control cells. Thereafter, mRNA levels of EGFR were assessed by qRT-PCR. As shown in Figures 4A and 4B, depletion of RUNX1 by siRNAs led to a significant decrease in EGFR mRNA levels in both Tsc2-null and Tsc1-null MEFs. Consistently, inhibition of RUNX1 by Ro5-3335 resulted in significantly reduced EGFR mRNA levels in these cells (Figures 4C and 4D). In contrast, ectopic

expression of RUNX1 markedly upregulated the expression of EGFR mRNA in $Tsc2^{+/+}$ MEFs (Figure 4E). These data together suggested that RUNX1 upregulates EGFR at the mRNA level.

To gain further insights into how RUNX1 controls the expression of EGFR mRNA, we analyzed the 5′-flanking sequence of the EGFR gene upstream of the transcription start site (TSS) using the Jaspar transcription profile database (http://jaspar.genereg.net). A putative RUNX1-binding sequence: R1 (−326/−316, CAACCACATGG) was identified in a 1.5-kb region upstream of the TSS of the mouse EGFR gene (Figure 4F). We then cloned the mouse EGFR gene promoter (−758 to +157 bp) into a luciferase reporter vector and evaluated the effect of RUNX1 on promoter activity. As shown in Figure 4G, the luciferase reporter assay performed in 293T cells showed a significant elevation of reporter signals upon additive expression of RUNX1. Furthermore, mutation of R1 reduced transcriptional activity, indicating that RUNX1 regulates EGFR transcription by binding to the R1 region (Figure 4G). Similar results were observed when luciferase reporter assays were performed in $Tsc2^{+/+}$ MEFs (Figure 4H). Next, by performing an anti-RUNX1 chromatin immunoprecipitation (ChIP) assay, we found that the recruitment of the RUNX1 protein to the R1 region was significantly enhanced in $Tsc2^{-/-}$ MEFs in comparison with $Tsc2^{+/+}$ MEFs (Figure 4I). Moreover, the binding was attenuated by the addition of rapamycin (Figure 4I). Together, these results indicate that RUNX1 directly interacts with the EGFR promoter and positively regulates its transcription.

The mTORC1/RUNX1/EGFR signaling pathway exists in human cancer cells

We next analyzed the correlation between EGFR expression and mTOR signaling pathway activity in cancer patients by gene set enrichment analysis using The Cancer Genome Atlas (TCGA) RNA-seq datasets. The results demonstrated that the genes positively regulated by mTOR signaling were enriched in EGFR-high expression groups in ovarian cancer, as well as in prostate adenocarcinoma (Figures 5A and 5B).

To further evaluate whether this newly discovered mTORC1 regulation of the RUNX1/EGFR pathway also occurs in human cancer cells, we employed two human cancer cell lines, SKOV3 (an ovarian cancer cell line) and DU145 (a prostate cancer cell line). As shown in Figure 5C, knockdown of the mTORC1-specific partner Raptor resulted in the significant downregulation of RUNX1 as well as EGFR in SKOV3 cells. Furthermore, depletion of Raptor led to a similar result in DU145 cells (Figure 5D), and suppression of RUNX1 by genetic or pharmacological strategies led to a significant decrease in EGFR expression in both SKOV3 and DU145 cells (Figures 5E–5H). Collectively, the mTORC1/RUNX1/EGFR signaling cascade was also detected in human cancer cells.

Elevated EGFR expression promotes cell proliferation and tumorigenicity of mTORC1-activated cells

To investigate the potential role of EGFR in cell growth, we infected Tsc2-null MEFs with lentiviruses expressing shRNA targeting EGFR (shEGFR) or a scrambled sequence (shSc). Western blot analysis verified that shEGFR dramatically decreased EGFR expression when compared with the shSc group (Figure 6A). As shown in Figure 6B, EGFR knockdown in the $Tsc2^{-/-}$/shEGFR group resulted in a marked decrease in cell proliferation rate compared with the $Tsc2^{-/-}$/shSc group. In addition, $Tsc1^{+/+}$ MEFs were transfected with an EGFR-encoding lentivirus ($Tsc1^{+/+}$/LvEGFR group) and control lentivirus ($Tsc1^{+/+}$/Lv group) (Figure 6C). In contrast to depletion of EGFR, EGFR overexpression led to an increased cell proliferation rate in the $Tsc1^{+/+}$/LvEGFR group compared with the $Tsc1^{+/+}$/Lv group (Figure 6D).

Next, we investigated the role of EGFR in cell growth *in vivo*. NTC/T2-null, a cell line with high tumorigenicity derived from a subcutaneous tumor formed by the injection of $Tsc2^{-/-}$ MEFs in nude mouse, was used.[17] EGFR shRNA-expressing NTC/T2-null and control cells (Figure S2) were subcutaneously injected into the right anterior armpit of nude mice and the tumor growth monitored thereafter. As demonstrated in Figures 6E–6G, depletion of EGFR significantly decreased the tumorigenic capacity of NTC/T2-null cells compared with the control. Reduced EGFR expression in the tumor tissues derived from mouse EGFR shRNA-expressing NTC/T2-null was verified by western blot (Figure 7D). In contrast, overexpression of EGFR dramatically enhanced the tumorigenic capacity of $Tsc1^{+/+}$ MEFs (Figures 6H–6J). Taken together, these results indicate that EGFR enhances cell proliferation and tumoral growth of mTORC1-activated cells.

mTORC1-mediated EGFR upregulation leads to activation of STAT3

Hyperactivated mTORC1 leads to the activation of STAT3; however, the underlying mechanism remains largely obscure.[18] Because STAT3 is a well-known downstream effector of EGFR,[8] we speculated that increased EGFR is, at least in part, responsible for the augmented STAT3 activity due to hyperactivation of mTORC1. To test this hypothesis, we starved $Tsc2^{-/-}$ MEFs with shEGFR and control cells for 24 h and then treated them with EGF for up to 15 min. As shown in Figure 7A, reduction of EGFR markedly attenuated STAT3 activation induced by EGF. Similarly, inhibition of EGFR by gefitinib treatment also significantly suppressed the activation of STAT3 in response to EGF in $Tsc2^{-/-}$ MEFs (Figure 7B). Moreover, EGF stimulation enhanced the activation of STAT3 induced by EGFR overexpression in $Tsc1^{+/+}$ MEFs (Figure 7C). Furthermore, a decreased level of p-STAT3 was observed in tumor tissues derived form shEGFR-expressing NTC/T2-null cells compared with the control tissues (Figure 7D). In contrast, elevated p-STAT3 expression in the tumor tissues derived from EGFR-overexpressing $Tsc1^{+/+}$ MEFs was observed by western blot (Figure 7E). In addition, immunohistochemical analysis showed that staining of p-STAT3 and proliferation marker Ki67 were more intense in tumor tissues that were overexpressing EGFR compared with the control (Figure 7F). Taken together, these findings reveal that EGFR is critical for STAT3 activation and that hyperactivated mTORC1 activates STAT3 partially through the upregulation of EGFR.

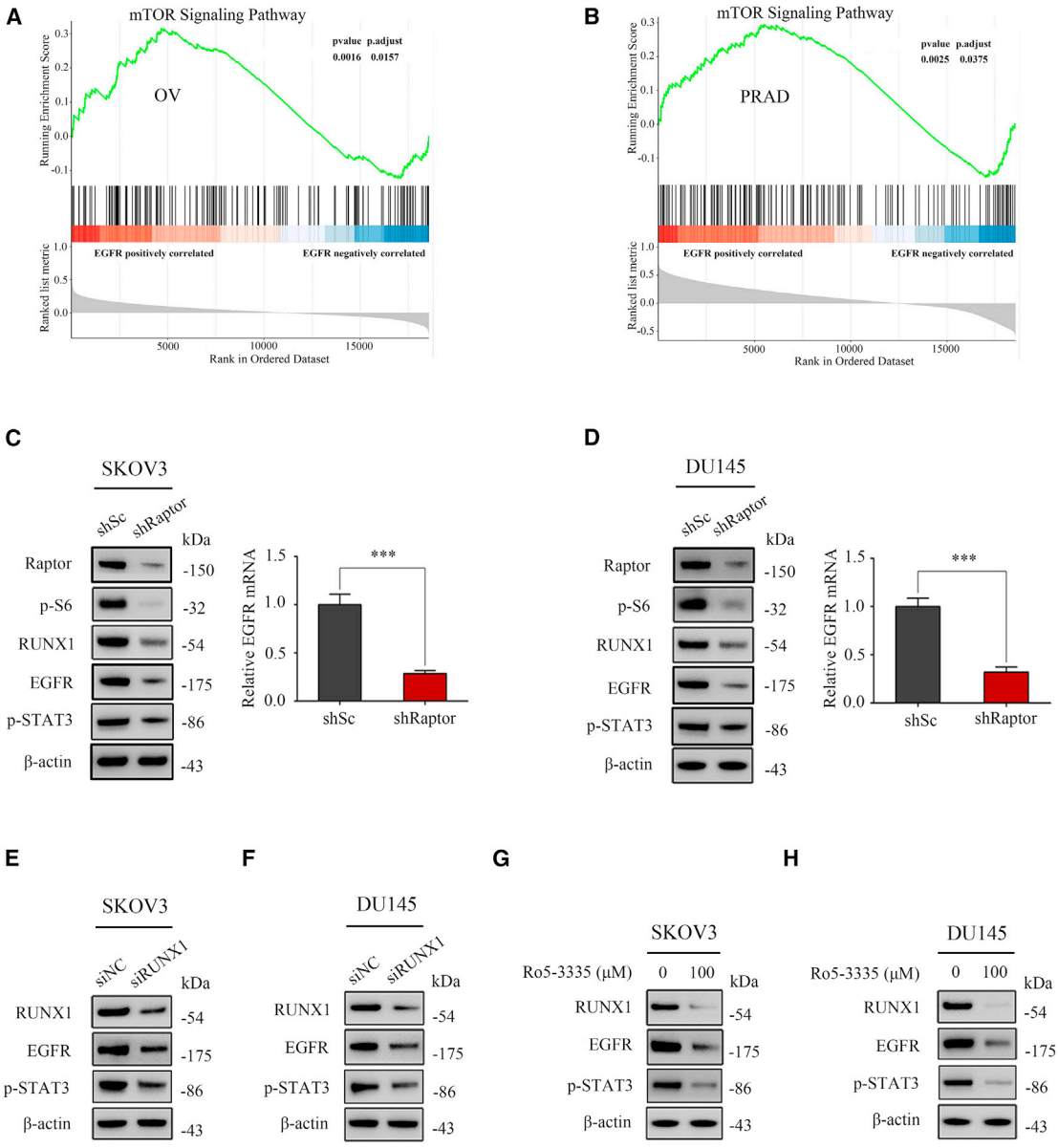

Figure 5. The mTORC1/RUNX1/EGFR signaling pathway exists in human cancer cells

(A and B) Gene set enrichment analysis comparing the gene sets positively regulated by mTOR signaling in EGFR-high and EGFR-low ovarian cancer (A) and prostate adenocarcinoma cancer (B). (C and D) SKOV3 or DU145 cells stably expressing shRNAs targeting Raptor (shRaptor) or a control shRNA (shSc). (E and F) SKOV3 or DU145 cells were transfected with siNC or siRNAs against RUNX1. (G and H) SKOV3 or DU145 cells were treated with or without Ro5-3335 (100 μM) for 24 h. In (C) to (H), cell lysates were subjected to immunoblotting with the indicated antibodies. qRT-PCR was performed to detect the mRNA level of EGFR (right panels of C and D). Error bars indicate mean ± SD of triplicate samples. ***$p < 0.001$.

Depletion of STAT3 blocks cell proliferation and tumor growth driven by EGFR overexpression

To further investigate whether the pro-proliferative effect of EGFR is mediated by STAT3, we transduced a lentiviral vector expressing shRNA for STAT3 to EGFR-overexpressing $Tsc2^{+/+}$ MEFs, and subsequent western blot analysis revealed that the shRNA for STAT3 dramatically suppressed the expression of STAT3 (Figure 8A). As shown in Figure 8B, depletion of STAT3 attenuated the accelerated cell proliferation driven by EGFR overexpression. A colony-formation assay was also employed to determine the long-term impact of STAT3 on cell proliferation driven by EGFR. We observed more colonies in the $Tsc2^{+/+}$/LvEGFR group than in the $Tsc2^{+/+}$/Lv group after 2 weeks, whereas decreased colony formation was observed in the shSTAT3-$Tsc2^{+/+}$/LvEGFR group (Figure 8C). Furthermore, we

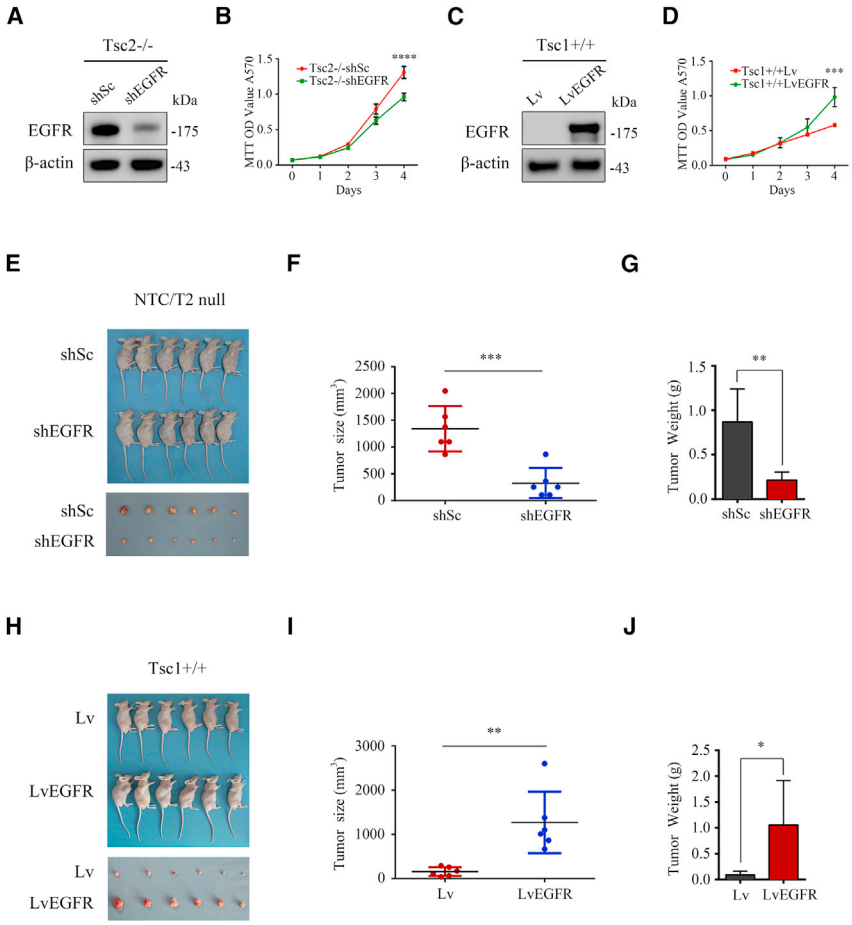

Figure 6. EGFR promotes oncogenic potential *in vitro* and *in vivo*

(A and B) Tsc2$^{-/-}$ MEFs stably expressing shRNAs targeting EGFR (shEGFR) or a control shRNA (shSc). (C and D) Tsc1$^{+/+}$ MEFs were infected with lentivirus harboring the GV367 vector encoding EGFR (LvEGFR) or the empty vector (Lv). (A and C) Cell lysates were subjected to immunoblotting with the indicated antibodies. (B and D) Proliferation of the indicated cells was examined using an MTT assay. (E–J) The indicated cells were inoculated subcutaneously into nude mice, followed by monitoring for tumor growth. (E and H) nude mice and tumor pictures. (F and I) Tumor volumes. (G and J) Tumor weight. Error bars indicate mean ± SD of triplicate samples. *p < 0.05, **p < 0.01, ***p < 0.001, ****p < 0.0001.

injected shSTAT3-Tsc2$^{+/+}$/LvEGFR, shSc-Tsc2$^{+/+}$/LvEGFR, and Tsc2$^{+/+}$/Lv MEFs subcutaneously into nude mice. As shown in Figures 8D–8F, depletion of STAT3 compromised the enhanced tumorigenic capacity driven by EGFR overexpression in Tsc2$^{+/+}$ MEFs. Moreover, EGFR and p-STAT3 expression status in the corresponding tumor tissues was verified by western blotting (Figure 8G). Taken together, these findings revealed that EGFR enhances the proliferative capacity of cells at least partially through the activation of STAT3.

DISCUSSION

Compelling evidence indicates that mTORC1 plays a crucial role in the development of tumors. TSC, a benign tumor syndrome in multiple organs, is caused by hyperactivated mTORC1 signaling due to loss-of-function mutations in the TSC1 or TSC2 gene.[19] Currently, the mTORC1 inhibitor rapamycin and its analogs are utilized for the treatment of TSC-related tumors, including angiomyolipomas, lymphangioleiomyomatosis, and subependymal giant cell astrocytomas.[20] However, the underlying mechanisms whereby hyperactivated mTORC1 leads to aberrant TSC tumor growth remain unclear. Immortalized Tsc1$^{-/-}$ and Tsc2$^{-/-}$ MEFs are well-established cell models for studying TSC and mTOR signaling.[21–23] Using these cell models, we have previously reported that hyperactivated mTORC1 fosters tumor growth by manipulating the expression of multiple glycolytic enzymes, such as PKM2, LDHB, and PFKFB3.[13,17,24,25] RTKs have been shown to be aberrantly expressed in many tumors, including TSC.[26] However, in addition to PDGFRα and PDGFRβ, information on other RTKs that contribute to the development of TSC tumors is limited. In the current investigation, based on the study of Tsc1-null or Tsc2-null MEFs and their corresponding control cells, we identified EGFR as a novel downstream molecule of mTORC1 that accelerates the *in vitro* and *in vivo* cell growth of Tsc1- or Tsc2-deficient cells. Moreover, we show that mTORC1 positively regulates EGFR expression in rat Tsc2-null cells and human cancer cells. These results together suggest that mTORC1 upregulation of EGFR is a common phenomenon across the species, and thus EGFR may be potentially utilized as a therapeutic target in TSC as well as in other mTORC1-related tumors. Previous studies support this hypothesis by demonstrating that anti-EGFR antibody exposure efficiently inhibits human Tsc2$^{-/-}$ smooth muscle cell proliferation[27] and decreases the number and dimension of lung nodules, and reverses pulmonary alterations in a mouse model of lymphangioleiomyomatosis.[28] Given that EGFR inhibitors are widely used in the treatment of cancer, it is worthwhile to explore the clinical anti-TSC tumor effects of EGFR inhibitors in the future.

EGFR plays a crucial role in the growth, differentiation, and motility of normal as well as cancer cells.[9] For predictive cancer diagnostics and therapeutic targeting of EGFR, it is critical to explore how EGFR expression is controlled. Recent studies have focused on the transcriptional regulation of EGFR. For example, Mizuguchi et al. reported that the transcription factor ecotropic viral integration site 1 (EVI1) induces the proliferation of glioblastoma cells through direct upregulation of EGFR.[29] Jin et al. demonstrated that the transcription growth factor β inducible early gene 1 (TIEG1) significantly inhibits breast cancer cell invasion and metastasis by inhibiting EGFR gene

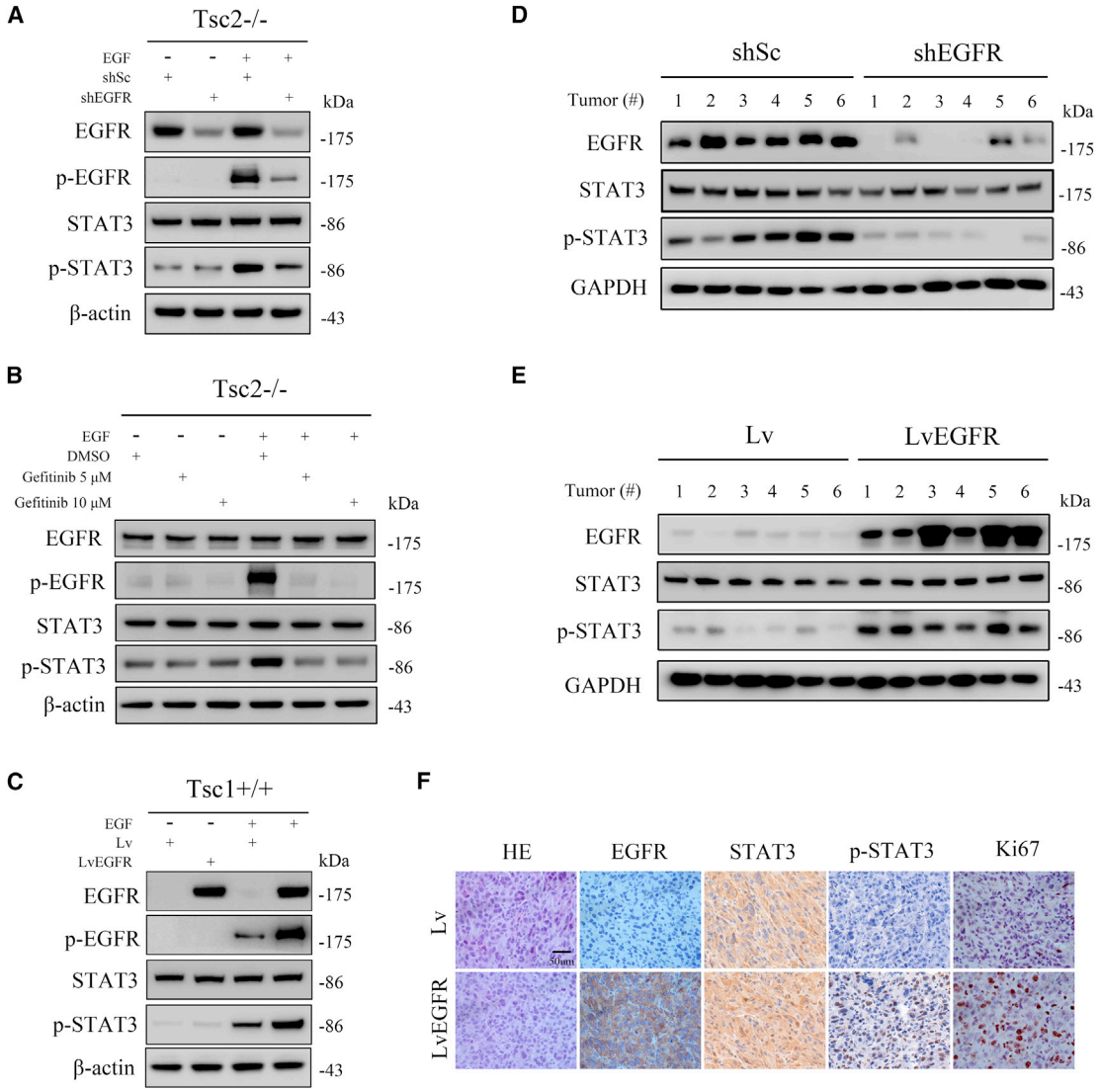

Figure 7. mTORC1-mediated EGFR upregulation leads to the activation of STAT3

(A) Tsc2$^{-/-}$ MEFs were infected with lentivirus expressing shRNAs targeting EGFR (shEGFR) or a control shRNA (shSc). (B) Tsc2$^{-/-}$ MEFs were pretreated with or without gefitinib (5 and 10 μM) for 24 h. (C) Tsc1$^{+/+}$ MEFs were transduced with LvEGFR or Lv lentiviruses. In (A) to (C), cells were starved in DMEM for 24 h, followed by stimulation with EGF (50 mg/mL, 15 min), after which cell lysates were harvested and subjected to western blot analysis. (D and E) Tumor tissues derived from Tsc2$^{-/-}$ shEGFR MEFs or Tsc1$^{+/+}$ LvEGFR MEFs and their corresponding control cells were subjected to immunoblotting. (F) Tumor tissues derived from Tsc1$^{+/+}$/LvEGFR and the control cells were fixed and embedded with paraffin and then subjected to H&E and immunohistochemical staining. Representative images are presented. Scale bar, 50 μm.

transcription.[30] In addition, other transcription factors, such as specificity protein 1 (Sp1), retinoic acid receptor γ (RARγ), AP-1 transcription factor subunit (c-Jun), homeobox B5 (HOXB5), cytoplasmic polyadenylation element binding protein 3 (CPEB3), and Y-box-binding protein 1 (YB-1) have also been shown to be involved in the regulation of EGFR transcription in different types of cells.[31–35] Here, based on the study of Tsc1-null or Tsc2-null MEFs and human cancer cell lines, we suggest that the transcription factor RUNX1, as a downstream effector of mTORC1, upregulates EGFR at the transcriptional level by directly binding to the promoter of the EGFR gene. Subsequently, upregulated EGFR accelerates cell proliferation and tumoral growth of Tsc1-null or Tsc2-null cells through activation of STAT3. We not only identified a new transcription factor of EGFR, but also revealed a signaling pathway, the RUNX1/EGFR/STAT3 pathway, by which dysregulated mTORC1 drives carcinogenesis. Hence, besides EGFR inhibitors, RUNX1 and STAT3 inhibitors or some DNA-binding compounds such as Py-Im polyamides, which target the binding sequences of RUNX1 or STAT3,[14,36] are also expected to have therapeutic value in treating mTORC1-related cancers. In addition, our result confirmed previous studies that delineated

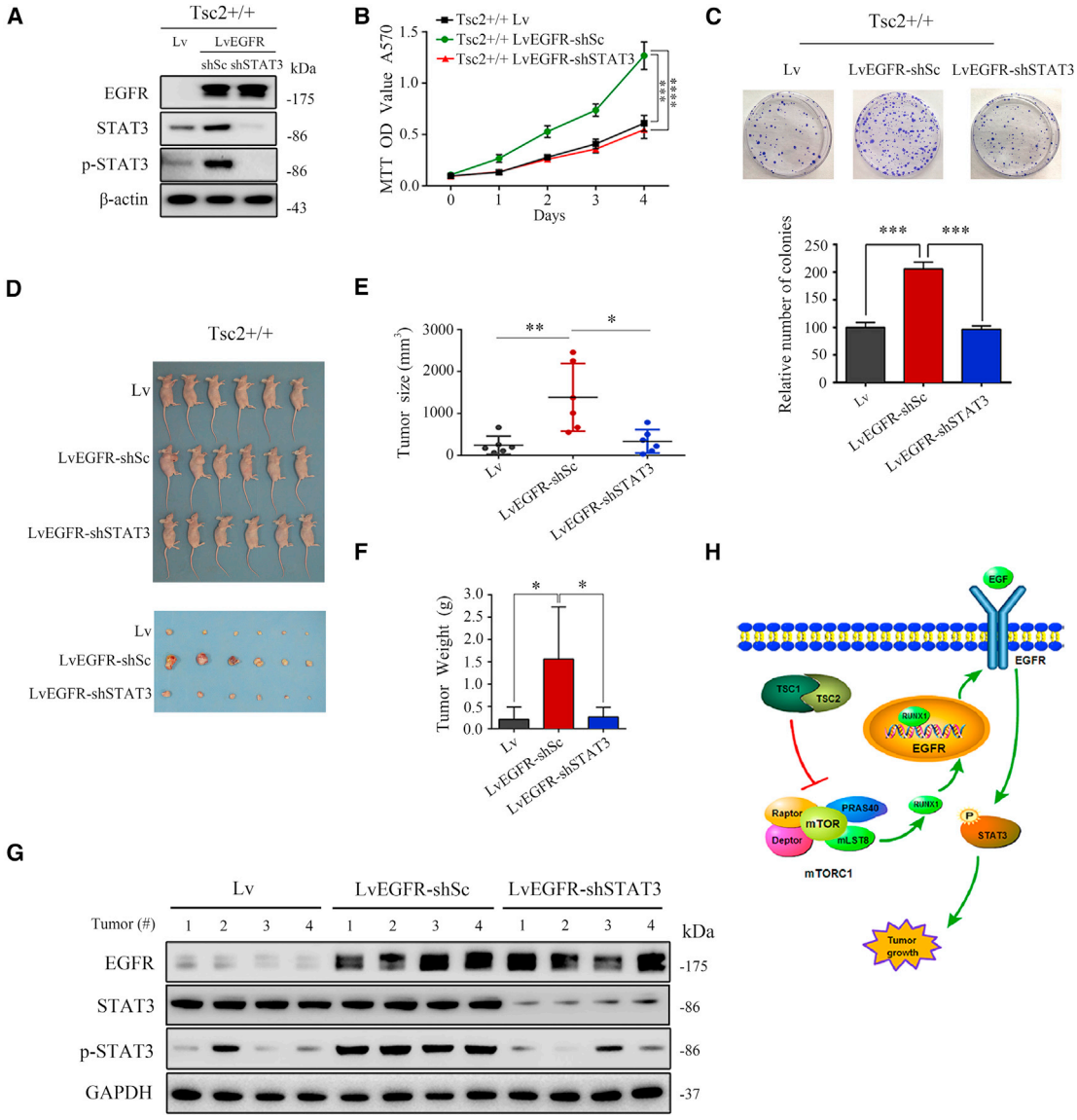

Figure 8. Depletion of STAT3 blocks EGFR overexpression-induced cell proliferation and tumor growth

(A–C) LvEGFR-expressing Tsc2$^{+/+}$ MEFs were infected with lentivirus harboring shSTAT3 or shSc. (A) Cell lysates were harvested and subjected to western blot analysis with the indicated antibodies. (B) The proliferation of the indicated cells was examined by an MTT assay. (C) The colonies formed by the indicated cells were stained and counted. Representative images (upper panels) and quantifications (lower panels). (D–G) LvEGFR-expressing Tsc2$^{+/+}$ MEFs transduced with shSTAT3 or shSc lentiviruses, and Tsc2$^{+/+}$ Lv MEFs were inoculated subcutaneously into nude mice, following by monitoring for tumor growth. At 27 days after inoculation, mice were sacrificed and photographed. (D) Nude mice and tumor pictures. (E) Tumor volumes. (F) Tumor weight. (G) Tumor tissues derived from the indicated cells were subjected to immunoblotting. (H) Schematic illustration of the TSC1/TSC2/mTORC1 signaling pathway-promoted tumor growth through the RUNX1/EGFR/STAT3 network. Error bars indicate mean ± SD of triplicate samples. *p < 0.05, **p < 0.01, ***p < 0.001, ****p < 0.0001.

RUNX1 as a downstream target of mTORC1.[37,38] However, the underlying mechanism of upregulation of RUNX1 by mTORC1 remains unclear. A recent study reported that the RNA-binding protein HuR can stabilize and promote the expression of RUNX1 by directly binding to RUNX1 mRNA.[39] Because mTORC1 can modulate the association between HuR and its target mRNAs,[40] it is possible that mTORC1 increases RUNX1 expression by enhancing the interaction of HuR with RUNX1 mRNA. However, further studies on this interaction are warranted.

STAT3 mediates a plethora of biological functions, including roles in cell proliferation, differentiation, apoptosis, and inflammation.[41] Growing evidence suggests that STAT3 is constitutively activated in a wide range of cancer types and plays a pivotal role in tumor expansion

and metastasis.[42] In response to cytokine or growth factor stimulation, STAT3 is phosphorylated at the Tyr705 residue, which facilitates its homodimerization and nuclear translocation.[42] The nucleus-accumulating STAT3 binds to specific DNA response elements and induces gene expression.[42] Additionally, STAT3 can be phosphorylated by numerous kinases on Ser727, a site that promotes its transcriptional activity.[43] It is widely perceived that STAT3 functions as a known downstream effector molecule of mTORC1 signaling. For example, Zhou and colleagues reported that the mTORC1/STAT3 pathway is required for the viability and the maintenance of breast cancer stem-like cells.[44] Yang et al. demonstrated that Gadd45a inhibits tumor angiogenesis by blocking the mTORC1/STAT3 signaling pathway.[45] Our previous study revealed that hyperactivated mTORC1 inhibits cell differentiation, upregulates glucose metabolism, and induces angiogenesis through phosphorylation and activation of STAT3.[17,21,46] Goncharova and colleagues also showed that treatment of Tsc2-null tumors with rapamycin attenuated STAT3 expression and phosphorylation, and reduction of STAT3 protein levels or activity decreased proliferation and induced apoptosis in Tsc2-null and lymphangioleiomyomatosis-dissociated (LAMD) cells.[47] However, the underlying mechanism by which mTORC1 activates STAT3 is poorly characterized. In this study, we found that inhibition of EGFR using either genetic or pharmacologic strategies attenuates STAT3 Tyr705 phosphorylation and activation in Tsc1- or Tsc2-deficient cells, while overexpression of EGFR facilitates the phosphorylation and activation of STAT3 (Figure 7). Moreover, knockdown of STAT3 disrupts the accelerated cell proliferation driven by the ectopic expression of EGFR both *in vitro* and *in vivo* (Figure 8). Thus, these findings provide the first evidence that mTORC1 activates STAT3, at least in part, by transactivating EGFR expression. Together with previous findings that mTORC1 upregulates STAT3 protein levels by virtue of the suppression of miR-125b-5p and that mTORC1 can phosphorylate STAT3 at Ser727,[48,49] these findings indicate that mTORC1 modulates STAT3 at multiple levels.

It must be pointed out that in addition to EGFR, our RNA-seq data suggest that other RTKs such as vascular endothelial growth factor receptor 2 (VEGFR2) and recepteur d'origine nantais (RON) were upregulated in $Tsc2^{-/-}$ MEFs as compared with $Tsc2^{+/+}$ MEFs. Western blot analysis showed that loss of TSC2 led to upregulation of RON, and its expression was decreased in response to rapamycin treatment (Figure S3). However, the expression of VEGFR2 was undetectable, probably due to its low expression level in $Tsc2^{-/-}$ or $Tsc2^{+/+}$ MEFs (Figure S3). Given that STAT3 is a downstream target of RON,[50] it is possible that RON is also involved in mTORC1-mediated tumorigenesis and STAT3 activation. We would like to further explore this possibility in the future.

In conclusion, we demonstrate that aberrantly activated mTORC1 contributes to cell proliferation and tumor growth of cells by upregulating the RUNX1/EGFR signaling pathway (Figure 8H). Furthermore, EGFR exhibits a pro-proliferative effect on mTORC1-activated cells by activating STAT3 (Figure 8H). Our findings help in the elucidation of the molecular mechanism by which dysregulated mTORC1 signaling drives tumorigenesis, indicating that the components in the RUNX1/EGFR/STAT3 pathway may be targeted for the treatment of TSC and other mTORC1-related tumors.

MATERIALS AND METHODS

Cell culture and treatment

All MEFs, including $Tsc1^{+/+}$, $Tsc1^{-/-}$, $Tsc2^{+/+}$, $Tsc2^{-/-}$, $Pten^{+/+}$, $Pten^{-/-}$, pLXIN or pLXIN-hTSC2 retrovirus-infected $Tsc2^{-/-}$ MEFs, pLXIN or pLXIN-myrAKT1 retrovirus-infected $Pten^{+/+}$ MEFs, rat uterine leiomyoma-derived Tsc2-null ELT3 cells, and NTC/T2-null cells have been described previously.[17,21,51,52] SKOV3, DU145, and HEK 293T cells were obtained from the ATCC (Manassas, VA, USA). ELT3 cells were maintained and propagated in DMEM/F12 (1:1) with 10% fetal bovine serum (FBS). SKOV3 and DU145 cells were maintained in 1640 medium supplemented with 10% FBS. The other cells were cultured in DMEM with 10% FBS. All cells were cultured at 37°C in a humidified incubator containing 5% CO_2. For drug treatment, cells were plated in 12-well plates at a density of 2×10^5 cells/well and cultured overnight. On day 2, the DMSO (Sigma-Aldrich, St. Louis, MO, USA) stocks of drugs were diluted to appropriate concentrations with the cell culture medium, and the cells treated for 24 h. Rapamycin and gefitinib were purchased from Selleck Chemicals (Houston, TX, USA). Ro5-3335 was obtained from TargetMol (Shanghai, China). For epidermal growth factor (EGF) stimulation, cells were treated with a bath application of EGF (Novus Biologicals, Littleton, CO, USA) for 15 min after serum starvation for 24 h. Cells were washed with 1× phosphate-buffered saline and harvested for qRT-PCR or western blot analyses as described below.

qRT-PCR

Total RNA was extracted from the cells using TRIzol reagent according the manufacturer's instructions. The concentration of isolated RNA was measured with NanoDrop (Thermo Fisher Scientific, Waltham, MA, USA). RNA (1 μg) was converted to first-strand cDNA using a RevertAid First Strand cDNA Synthesis Kit (Fermetas, Waltham, MA, USA). The cDNA was diluted 10× and used as the template for the reaction of qRT-PCR using SYBR Premix Ex Taq II (TaKaRa, Shiga, Japan) on the Bio-Rad CFX96 system (Bio-Rad, Hercules, CA, USA). The results were analyzed by comparing the Ct value based on the expression of housekeeping gene β-actin. The primer sequences are as follows: EGFR (mouse) forward: 5′-CAG CAT GTG GCA CCA TCT CA-3′ and reverse: 5′-AAA GCA GAA ACT CAC ATC GA-3′; EGFR (human) forward: 5′-AGG CAC GAG TAA CAA GCT CAC-3′ and reverse: 5′-ATG AGG ACA TAA CCA GCC ACC-3′; β-actin (mouse) forward: 5′-AGA GGG AAA TCG TGC GTG AC-3′ and reverse: 5′-CAA TAG TGA TGA CCT GGC CGT-3′; β-actin (human) forward: 5′-CCC TGG AGA AGA GCT ACG AG-3′ and reverse: 5′-GGA AGG AAG GCT GGA AGA GT-3′.

Western blot

Membrane proteins were isolated using the Membrane and Cytosol Protein Extraction Kit (Beyotime Biotechnology, Haimen, China). Total cellular, membrane, or tissue proteins were extracted by RIPA buffer

(Beyotime Biotechnology) and then separated by NuPAGE 10% or 4%–12% Bis-Tris gels (Life Technologies, Carlsbad, CA, USA), following the transfer to PVDF membrane (Millipore, Billerica, MA, USA). The membranes were blocked with 5% nonfat milk in 1× Tris-buffered saline with 0.1% Tween 20 (TBST) for 1 h at room temperature, and incubated thereafter with the specific primary antibody overnight at 4°C. Antibodies specific to TSC1 (#6935), TSC2 (#4308), p-EGFR (Tyr1068) (#3777), EGFR (#4267), Raptor (#2280), Rictor (#2114), PTEN (#9559), p-AKT (Ser473) (#4051), AKT1 (#2967), p-STAT3 (Tyr705) (#9145), STAT3 (#9139), p-S6 (Ser235/236) (#4857), Na,K-ATPase (#3010), Ki67 (#12202), GAPDH (#2218), and β-actin (#4970) were obtained from Cell Signaling Technology (Danvers, MA, USA). RUNX1 (ab35962) and VEGFR2 (ab221679) antibodies were obtained from Abcam (London, UK). RON (11053) antibodies were obtained from Proteintech (Wuhan, China). After washing with TBST, the membranes were incubated with HRP-labeled secondary antibodies (Cell Signaling Technology). The bands were visualized using Pierce ECL Western Blotting Substrate (Advansta, Menlo Park, CA, USA) according to the manufacturer's instructions.

RNA interference

All the siRNA oligonucleotides were synthesized by GenePharma (Shanghai, China). siRNA transfection was carried out in cells cultured in a 12-well plate at 50%–70% confluence. Cells were transfected with siRNAs by Lipofectamine 2000 (Invitrogen, Carlsbad, CA, USA) according to the manufacturer's instructions. The target sequences are listed as follows: Negative control (NC), 5′-UUC UCC GAA GGU GUC ACG U-3′; RUNX1^{-1} (mouse), 5′-CGC CCU CCU ACC AUC UAU A-3′; RUNX1^{-2} (mouse), 5′-GCA GAA CUG AGA AAU GCU A-3′; RUNX1 (human), 5′-GGC AGA AAC UAG AUG AUC A-3′.

Lentiviral transduction

GV358 lentiviral plasmid expressing mouse EGFR, RUNX1, and the empty vector were purchased from GeneChem (Shanghai, China). The GV248 lentiviral shRNA expression vector targeting Raptor, Rictor, EGFR, STAT3, and the control scrambled shRNA (shSc) were obtained from GenePharma. The target sequences were as follows: shRaptor (mouse), 5′-GGA CAA CGG TCA CAA GTA C-3′; shRaptor (human), 5′-GGA CAA CGG CCA CAA GUA C-3′; shRictor (mouse), 5′-GCC CTA CAG CCT TCA TTT A-3′; shEGFR, 5′-GTG CTA CGC AAA CAC AAT A-3′; shSTAT3, 5′-CTG GAT AAC TTC ATT AGC A-3′; shSc, 5′-TTC TCC GAA CGT GTC ACG T-3′. Lentiviruses were generated by co-transfecting with either of the recombinant vectors or the control vectors together with packaging vectors (pVSVG and psPAX2) into HEK 293T cells. At 48–72 h after infection the culture supernatants were collected and filtered, then used to infect target cells with a multiplicity of infection of 20–50. Stable clone cells were selected using 5 μg/mL puromycin (Sigma-Aldrich) for 7 days and verified by western blot.

Reporter constructs and luciferase reporter assay

A 913-bp fragment of the mouse EGFR promoter (−758/+157) was amplified by PCR using genomic DNA extracted from Tsc2$^{-/-}$ MEFs. The fragments were cloned into luciferase reporter gene vector pGL3-Basic (Promega, Madison, WI, USA) plasmid at the *Kpn*I/*Bgl*II site to generate a recombinant plasmid pEGFR-Luc. The primer sequences used for PCR were as follows: forward, 5′-GGG GTA CCG GTG ATG ATC TTG AGG AG-3′; reverse, 5′-CCG AGA TCT ACT CCA CGG TGT AAC AGC-3′. To generate a mutated promoter construct pEGFR$_{mut}$-Luc, we mutated the potential RUNX1-binding site on the promoter of the mouse EGFR gene using the Q5 site-directed mutagenesis kit (NEB, Ipswich, MA, USA). The primer sequences were as follows: forward, 5′-CAG CAA GTC TAT GGT GGC TCA CAA C-3'; reverse, 5′-GGA TTT GAA CTC CGG ACC TTC GGA AG-3′. Cells were seeded into 24-well culture plates on the day before transfection. For luciferase reporter assays, cells were transfected with 500 ng of pEGFR-Luc or pEGFR$_{mut}$-Luc together with 20 ng of internal control plasmid pRL-TK and 500 ng of RUNX1-encoding plasmids (#14585, Addgene, Watertown, MA, USA) or the empty vector pcDNA3.1 (Invitrogen). The luciferase activity was detected using the Dual-Luciferase Reporter Assay System (Promega), according to the manufacturer's instructions, with EnSpire (PerkinElmer, Waltham, MA, USA), and the raw data are provided in Table S2.

Chromatin immunoprecipitation

The ChIP assay was performed using a SimpleChIP Plus Enzymatic Chromatin IP kit (Cell Signaling Technology) with anti-RUNX1 antibody (ab23980, Abcam) according to the manufacturer's instructions. The released DNA was purified and analyzed by qRT-PCR. The primer sequences for PCR were as follows: the putative RUNX1-binding region (PBR), forward 5′-CAC CCG ACT GCT CTT CCG AAG GT-3′, reverse 5′-CTG TAG CCG TCT TCA GAC ACT CCA G-3′; a nonspecific RUNX1-binding region (NBR), forward 5′-CTG GCA TAG ATT GGC TGG ACT TCC-3′, reverse 5′-GGC CAC CAC TAG ACA AGG CTC TG-3′.

Cell proliferation assay

Cells were cultured in 96-well plates in triplicate at a density of 1,500 cells/well and incubated for 24, 48, 72, or 96 h. Cell proliferation was measured using the 3-(4,5-dimethylthiazol-2-yl)-2, 5-diphenyltetrazolium bromide (MTT; Beyotime, Haimen, China) assay as previously described.[13]

Cloning formation assay

Cells were seeded into 10-cm-diameter cell culture dishes at a density of 500 cells per dish. After incubation for about 10 days, the cells were fixed with methanol for 15 min and stained with 0.1% crystal violet (1 mg/mL, Sigma) for 20 min. The number of colonies with over 50 cells was counted.

Induction of subcutaneous tumor formation in nude mice

All experimental immunodeficient 5-week-old male BALB/c nude mice (weight 16–18 g) were purchased from Vital River Laboratories Animal Technology (Beijing, China). Six nude mice were randomly used in each cohort. Cells were mixed with 0.2 mL of DMEM and injected subcutaneously into the right anterior armpit of mice, after

which mouse growth and tumor formation were monitored every 3 days. To evaluate the role of EGFR in the *in vivo* growth of Tsc-deficient cells, mice were sacrificed and imaged on day 29 following inoculation of 4×10^6 NTC/T2-null expressing shEGFR or shSc and on day 27 following inoculation of 6×10^6 $Tsc1^{+/+}$/Lv or $Tsc1^{+/+}$/LvEGFR. To evaluate the function of STAT3 in the *in vivo* growth of EGFR-overexpressing cells, 6×10^6 shSTAT3-$Tsc2^{+/+}$/LvEGFR, shSc-$Tsc2^{+/+}$/LvEGFR, and $Tsc2^{+/+}$/Lv MEFs were subcutaneously inoculated into each group of mice, and after 27 days all the mice were anesthetized and sacrificed. Tumor dimensions were measured with a digital caliper, and tumor volume was calculated using the equation $V = 1/2(\text{width}2 \times \text{length})$. The tumor tissues were homogenized in RIPA buffer or fixed with 10% formalin for further studies after weighing. All animals were maintained and used in strict accordance with the guidelines of the Animal Center of Anhui Medical University.

Immunohistochemical analysis

Tumor tissues fixed with 4% paraformaldehyde were embedded in paraffin. The samples were sliced into 4-μm-thick sections. For histological examination, sections were deparaffinized and subjected to hematoxylin and eosin (H&E) staining. For immunohistochemical analysis, after deparaffinization the following primary antibodies were used for immunohistochemical staining: EGFR, Ki67, and p-STAT3 (Tyr705) (Cell Signaling Technology). The sections were then incubated with HRP-conjugated secondary antibody for 30 min and treated with a DAB Substrate Kit (Sigma-Aldrich).

RNA sequencing

$Tsc2^{-/-}$ and $Tsc2^{+/+}$ MEFs were harvested for RNA extraction with TRIzol reagent (Invitrogen). Gene expression profiles were determined by next-generation sequencing with an Illumina Nova-Seq (KangCheng Bio-Tech, Shanghai, China). Genes with changes in expression of 2.0-fold or more ($p < 0.05$) were considered to be differentially expressed. The list of differentially expressed genes is provided in Table S3.

Bioinformatics analysis

RNA-seq data from patients with ovarian cancer (n = 374) and prostate cancer (n = 498) were obtained from TCGA (http://cancergenome.nih.gov/). Gene set enrichment analysis was performed to examine the enrichment of mTOR positively regulated gene sets in EGFR-high and EGFR-low ovarian cancer and prostate cancer tissues according to previously described methods.[53] The expression association between EGFR and RUNX1 in tumor tissues was investigated using GEPIA (http://gepia.cancer-pku.cn/index.html).[54]

Statistical analysis

All data followed a normal distribution, and variance was similar among the groups that were statistically compared. Two-tailed Student's t test was used to compare the difference between two groups. One-way ANOVA was used to compare the differences in the experiments with more than two groups. The results are presented as the mean ± SD from at least triplicate samples. All statistical analyses were performed using GraphPad Prism 6.0 software. Differences were considered significant when $p < 0.05$.

ETHICS STATEMENT

All animal experiments were approved by the Experimental Animal Ethical Committee of Anhui Medical University.

SUPPLEMENTAL INFORMATION

Supplemental information can be found online at https://doi.org/10.1016/j.omto.2021.10.009.

ACKNOWLEDGMENTS

We thank Bao Li (School of Basic Medicine, Anhui Medical University) for the technical guidance of immunohistochemical staining. This work was supported by the Natural Science Foundation of China (81372475), Anhui Provincial Natural Science Foundation (1808085MH261), the Key Program in the Youth Elite Support Plan in Universities of Anhui Province (gxyqZD2017022), the Natural Science Foundation of Universities of Anhui Province (KJ2019A0219), the Natural Science Foundation of Anhui Medical University (2020xkj153), and 2020 Basic and Clinical Cooperative Research Promotion Program of Anhui Medical University (2020xkjT014).

AUTHOR CONTRIBUTIONS

Conception and design, W.L., X.W., J.H., and X.Z.; development of methodology, W.L., X.W., A.S., and J.H.; acquisition of data, W.L., X.W., A.S., M.Z., Xu Chen, Y.L., Z.W., H.H., and H.L.; analysis and interpretation of data, W.L., X.W., A.S., Xianguo Chen, and X.Z.; writing and review of the manuscript, W.L., X.W., and X.Z.; study supervision, J.H. and X.Z.

DECLARATION OF INTERESTS

The authors declare no competing interests.

REFERENCES

1. Liu, G.Y., and Sabatini, D.M. (2020). mTOR at the nexus of nutrition, growth, ageing and disease. Nat. Rev. Mol. Cell Biol. *21*, 183–203. https://doi.org/10.1038/s41580-019-0199-y.

2. Yi, J., Zhu, J., Wu, J., Thompson, C.B., and Jiang, X. (2020). Oncogenic activation of PI3K-AKT-mTOR signaling suppresses ferroptosis via SREBP-mediated lipogenesis. Proc. Natl. Acad. Sci. U S A *117*, 31189–31197. https://doi.org/10.1073/pnas.2017152117.

3. Mossmann, D., Park, S., and Hall, M.N. (2018). mTOR signalling and cellular metabolism are mutual determinants in cancer. Nat. Rev. Cancer *18*, 744–757. https://doi.org/10.1038/s41568-018-0074-8.

4. Switon, K., Kotulska, K., Janusz-Kaminska, A., Zmorzynska, J., and Jaworski, J. (2016). Tuberous sclerosis complex: from molecular biology to novel therapeutic approaches. IUBMB Life *68*, 955–962. https://doi.org/10.1002/iub.1579.

5. Inoki, K., Li, Y., Zhu, T., Wu, J., and Guan, K.L. (2002). TSC2 is phosphorylated and inhibited by Akt and suppresses mTOR signalling. Nat. Cell Biol. *4*, 648–657. https://doi.org/10.1038/ncb839.

6. Chong-Kopera, H., Inoki, K., Li, Y., Zhu, T., Garcia-Gonzalo, F.R., Rosa, J.L., and Guan, K.L. (2006). TSC1 stabilizes TSC2 by inhibiting the interaction between

TSC2 and the HERC1 ubiquitin ligase. J. Biol. Chem. *281*, 8313–8316. https://doi.org/10.1074/jbc.C500451200.

7. Kim, J., and Guan, K.L. (2019). mTOR as a central hub of nutrient signalling and cell growth. Nat. Cell Biol. *21*, 63–71. https://doi.org/10.1038/s41556-018-0205-1.
8. Wee, P., and Wang, Z. (2017). Epidermal growth factor receptor cell proliferation signaling pathways. Cancers (Basel) *9*, 5. https://doi.org/10.3390/cancers9050052.
9. Ayati, A., Moghimi, S., Salarinejad, S., Safavi, M., Pouramiri, B., and Foroumadi, A. (2020). A review on progression of epidermal growth factor receptor (EGFR) inhibitors as an efficient approach in cancer targeted therapy. Bioorg. Chem. *99*, 103811. https://doi.org/10.1016/j.bioorg.2020.103811.
10. Saraon, P., Pathmanathan, S., Snider, J., Lyakisheva, A., Wong, V., and Stagljar, I. (2021). Receptor tyrosine kinases and cancer: oncogenic mechanisms and therapeutic approaches. Oncogene *40*, 4079–4093. https://doi.org/10.1038/s41388-021-01841-2.
11. Zhang, H., Bajraszewski, N., Wu, E., Wang, H., Moseman, A.P., Dabora, S.L., Griffin, J.D., and Kwiatkowski, D.J. (2007). PDGFRs are critical for PI3K/Akt activation and negatively regulated by mTOR. J. Clin. Invest. *117*, 730–738. https://doi.org/10.1172/JCI28984.
12. Wang, L., Ni, Z., Liu, Y., Ji, S., Jin, F., Jiang, K., Ma, J., Ren, C., Zhang, H., Hu, Z., and Zha, X. (2017). Hyperactivated mTORC1 downregulation of FOXO3a/PDGFRalpha/AKT cascade restrains tuberous sclerosis complex-associated tumor development. Oncotarget *8*, 54858–54872. https://doi.org/10.18632/oncotarget.18963.
13. Zha, X., Hu, Z., Ji, S., Jin, F., Jiang, K., Li, C., Zhao, P., Tu, Z., Chen, X., Di, L., et al. (2015). NFkappaB up-regulation of glucose transporter 3 is essential for hyperactive mammalian target of rapamycin-induced aerobic glycolysis and tumor growth. Cancer Lett. *359*, 97–106. https://doi.org/10.1016/j.canlet.2015.01.001.
14. Morita, K., Suzuki, K., Maeda, S., Matsuo, A., Mitsuda, Y., Tokushige, C., Kashiwazaki, G., Taniguchi, J., Maeda, R., Noura, M., et al. (2017). Genetic regulation of the RUNX transcription factor family has antitumor effects. J. Clin. Invest. *127*, 2815–2828. https://doi.org/10.1172/JCI91788.
15. Mitsuda, Y., Morita, K., Kashiwazaki, G., Taniguchi, J., Bando, T., Obara, M., Hirata, M., Kataoka, T.R., Muto, M., Kaneda, Y., et al. (2018). RUNX1 positively regulates the ErbB2/HER2 signaling pathway through modulating SOS1 expression in gastric cancer cells. Sci. Rep. *8*, 6423. https://doi.org/10.1038/s41598-018-24969-w.
16. Boregowda, R.K., Medina, D.J., Markert, E., Bryan, M.A., Chen, W., Chen, S., Rabkin, A., Vido, M.J., Gunderson, S.I., Chekmareva, M., et al. (2016). The transcription factor RUNX2 regulates receptor tyrosine kinase expression in melanoma. Oncotarget *7*, 29689–29707. https://doi.org/10.18632/oncotarget.8822.
17. Zha, X., Wang, F., Wang, Y., He, S., Jing, Y., Wu, X., and Zhang, H. (2011). Lactate dehydrogenase B is critical for hyperactive mTOR-mediated tumorigenesis. Cancer Res. *71*, 13–18. https://doi.org/10.1158/0008-5472.CAN-10-1668.
18. Laplante, M., and Sabatini, D.M. (2013). Regulation of mTORC1 and its impact on gene expression at a glance. J. Cell Sci. *126*, 1713–1719. https://doi.org/10.1242/jcs.125773.
19. Crino, P.B., Nathanson, K.L., and Henske, E.P. (2006). The tuberous sclerosis complex. N. Engl. J. Med. *355*, 1345–1356. https://doi.org/10.1056/NEJMra055323.
20. Salussolia, C.L., Klonowska, K., Kwiatkowski, D.J., and Sahin, M. (2019). Genetic etiologies, diagnosis, and treatment of tuberous sclerosis complex. Annu. Rev. Genomics Hum. Genet. *20*, 217–240. https://doi.org/10.1146/annurev-genom-083118-015354.
21. Ma, J., Meng, Y., Kwiatkowski, D.J., Chen, X., Peng, H., Sun, Q., Zha, X., Wang, F., Wang, Y., Jing, Y., et al. (2010). Mammalian target of rapamycin regulates murine and human cell differentiation through STAT3/p63/Jagged/Notch cascade. J. Clin. Invest. *120*, 103–114. https://doi.org/10.1172/JCI37964.
22. Ben-Sahra, I., Hoxhaj, G., Ricoult, S.J.H., Asara, J.M., and Manning, B.D. (2016). mTORC1 induces purine synthesis through control of the mitochondrial tetrahydrofolate cycle. Science *351*, 728–733. https://doi.org/10.1126/science.aad0489.
23. Wu, R., Dang, F., Li, P., Wang, P., Xu, Q., Liu, Z., Li, Y., Wu, Y., Chen, Y., and Liu, Y. (2019). The circadian protein Period2 suppresses mTORC1 activity via recruiting Tsc1 to mTORC1 complex. Cell Metab. *29*, 653–667.e6. https://doi.org/10.1016/j.cmet.2018.11.006.
24. Sun, Q., Chen, X., Ma, J., Peng, H., Wang, F., Zha, X., Wang, Y., Jing, Y., Yang, H., Chen, R., et al. (2011). Mammalian target of rapamycin up-regulation of pyruvate kinase isoenzyme type M2 is critical for aerobic glycolysis and tumor growth. Proc. Natl. Acad. Sci. U S A *108*, 4129–4134. https://doi.org/10.1073/pnas.1014769108.
25. Wang, Y., Tang, S., Wu, Y., Wan, X., Zhou, M., Li, H., and Zha, X. (2020). Upregulation of 6-phosphofructo-2-kinase (PFKFB3) by hyperactivated mammalian target of rapamycin complex 1 is critical for tumor growth in tuberous sclerosis complex. IUBMB Life *72*, 965–977. https://doi.org/10.1002/iub.2232.
26. Regad, T. (2015). Targeting RTK signaling pathways in cancer. Cancers (Basel) *7*, 1758–1784. https://doi.org/10.3390/cancers7030860.
27. Lesma, E., Grande, V., Ancona, S., Carelli, S., Di Giulio, A.M., and Gorio, A. (2008). Anti-EGFR antibody efficiently and specifically inhibits human $TSC2^{-/-}$ smooth muscle cell proliferation. Possible treatment options for TSC and LAM. PLoS One *3*, e3558. https://doi.org/10.1371/journal.pone.0003558.
28. Lesma, E., Chiaramonte, E., Ancona, S., Orpianesi, E., Di Giulio, A.M., and Gorio, A. (2015). Anti-EGFR antibody reduces lung nodules by inhibition of EGFR-pathway in a model of lymphangioleiomyomatosis. Biomed. Res. Int. *2015*, 315240. https://doi.org/10.1155/2015/315240.
29. Mizuguchi, A., Yamashita, S., Yokogami, K., Morishita, K., and Takeshima, H. (2019). Ecotropic viral integration site 1 regulates EGFR transcription in glioblastoma cells. J. Neurooncol. *145*, 223–231. https://doi.org/10.1007/s11060-019-03310-z.
30. Jin, W., Chen, B.B., Li, J.Y., Zhu, H., Huang, M., Gu, S.M., Wang, Q.Q., Chen, J.Y., Yu, S., Wu, J., and Shao, Z.M. (2012). TIEG1 inhibits breast cancer invasion and metastasis by inhibition of epidermal growth factor receptor (EGFR) transcription and the EGFR signaling pathway. Mol. Cell Biol. *32*, 50–63. https://doi.org/10.1128/MCB.06152-11.
31. Zheng, Z.S., Polakowska, R., Johnson, A., and Goldsmith, L.A. (1992). Transcriptional control of epidermal growth factor receptor by retinoic acid. Cell Growth Differ. *3*, 225–232.
32. Peng, S.C., Lai, Y.T., Huang, H.Y., Huang, H.D., and Huang, Y.S. (2010). A novel role of CPEB3 in regulating EGFR gene transcription via association with Stat5b in neurons. Nucleic Acids Res. *38*, 7446–7457. https://doi.org/10.1093/nar/gkq634.
33. Lee, J.Y., Kim, J.M., Jeong, D.S., and Kim, M.H. (2018). Transcriptional activation of EGFR by HOXB5 and its role in breast cancer cell invasion. Biochem. Biophys. Res. Commun. *503*, 2924–2930. https://doi.org/10.1016/j.bbrc.2018.08.071.
34. Stratford, A.L., Habibi, G., Astanehe, A., Jiang, H., Hu, K., Park, E., Shadeo, A., Buys, T.P., Lam, W., Pugh, T., et al. (2007). Epidermal growth factor receptor (EGFR) is transcriptionally induced by the Y-box binding protein-1 (YB-1) and can be inhibited with Iressa in basal-like breast cancer, providing a potential target for therapy. Breast Cancer Res. *9*, R61. https://doi.org/10.1186/bcr1767.
35. Brandt, B., Meyer-Staeckling, S., Schmidt, H., Agelopoulos, K., and Buerger, H. (2006). Mechanisms of EGFR gene transcription modulation: relationship to cancer risk and therapy response. Clin. Cancer Res. *12*, 7252–7260. https://doi.org/10.1158/1078-0432.CCR-06-0626.
36. Wang, M., Ma, X., Zhou, K., Mao, H., Liu, J., Xiong, X., Zhao, X., Narva, S., Tanaka, Y., Wu, Y., et al. (2021). Discovery of pyrrole-imidazole polyamides as PD-L1 expression inhibitors and their anticancer activity via immune and nonimmune pathways. J. Med. Chem. *64*, 6021–6036. https://doi.org/10.1021/acs.jmedchem.1c00120.
37. Zhang, C., Wang, S., Li, J., Zhang, W., Zheng, L., Yang, C., Zhu, T., and Rong, R. (2017). The mTOR signal regulates myeloid-derived suppressor cells differentiation and immunosuppressive function in acute kidney injury. Cell Death Dis. *8*, e2695. https://doi.org/10.1038/cddis.2017.86.
38. Zhou, S., Zhang, L., Feng, D., Luo, M., Xie, R., Yang, K., Xu, D., Yang, K., Fei, J., and Zhou, T. (2019). The mTOR-RUNX1 pathway regulates DC-SIGN expression in renal tubular epithelial cells. Biochem. Biophys. Res. Commun. *519*, 620–625. https://doi.org/10.1016/j.bbrc.2019.09.042.
39. Chen, J., Martindale, J.L., Abdelmohsen, K., Kumar, G., Fortina, P.M., Gorospe, M., Rostami, A., and Yu, S. (2020). RNA-binding protein HuR promotes Th17 cell differentiation and can be targeted to reduce autoimmune neuroinflammation. J. Immunol. *204*, 2076–2087. https://doi.org/10.4049/jimmunol.1900769.
40. Origanti, S., Nowotarski, S.L., Carr, T.D., Sass-Kuhn, S., Xiao, L., Wang, J.Y., and Shantz, L.M. (2012). Ornithine decarboxylase mRNA is stabilized in an mTORC1-dependent manner in Ras-transformed cells. Biochem. J. *442*, 199–207. https://doi.org/10.1042/BJ20111464.

41. Guanizo, A.C., Fernando, C.D., Garama, D.J., and Gough, D.J. (2018). STAT3: a multifaceted oncoprotein. Growth Factors *36*, 1–14. https://doi.org/10.1080/08977194.2018.1473393.

42. Yu, H., Lee, H., Herrmann, A., Buettner, R., and Jove, R. (2014). Revisiting STAT3 signalling in cancer: new and unexpected biological functions. Nat. Rev. Cancer *14*, 736–746. https://doi.org/10.1038/nrc3818.

43. Wakahara, R., Kunimoto, H., Tanino, K., Kojima, H., Inoue, A., Shintaku, H., and Nakajima, K. (2012). Phospho-Ser727 of STAT3 regulates STAT3 activity by enhancing dephosphorylation of phospho-Tyr705 largely through TC45. Genes Cells *17*, 132–145. https://doi.org/10.1111/j.1365-2443.2011.01575.x.

44. Zhou, J., Wulfkuhle, J., Zhang, H., Gu, P., Yang, Y., Deng, J., Margolick, J.B., Liotta, L.A., Petricoin, E., 3rd, and Zhang, Y. (2007). Activation of the PTEN/mTOR/STAT3 pathway in breast cancer stem-like cells is required for viability and maintenance. Proc. Natl. Acad. Sci. U S A *104*, 16158–16163. https://doi.org/10.1073/pnas.0702596104.

45. Yang, F., Zhang, W., Li, D., and Zhan, Q. (2013). Gadd45a suppresses tumor angiogenesis via inhibition of the mTOR/STAT3 protein pathway. J. Biol. Chem. *288*, 6552–6560. https://doi.org/10.1074/jbc.M112.418335.

46. Hu, Z., Wang, Y., Huang, F., Chen, R., Li, C., Wang, F., Goto, J., Kwiatkowski, D.J., Wdzieczak-Bakala, J., Tu, P., et al. (2015). Brain-expressed X-linked 2 is pivotal for hyperactive mechanistic target of rapamycin (mTOR)-mediated tumorigenesis. J. Biol. Chem. *290*, 25756–25765. https://doi.org/10.1074/jbc.M115.665208.

47. Goncharova, E.A., Goncharov, D.A., Damera, G., Tliba, O., Amrani, Y., Panettieri, R.A., Jr., and Krymskaya, V.P. (2009). Signal transducer and activator of transcription 3 is required for abnormal proliferation and survival of TSC2-deficient cells: relevance to pulmonary lymphangioleiomyomatosis. Mol. Pharmacol. *76*, 766–777. https://doi.org/10.1124/mol.109.057042.

48. Zhang, C., Wan, X., Tang, S., Li, K., Wang, Y., Liu, Y., Sha, Q., Zha, X., and Liu, Y. (2020). miR-125b-5p/STAT3 pathway regulated by mTORC1 plays a critical role in promoting cell proliferation and tumor growth. J. Cancer *11*, 919–931. https://doi.org/10.7150/jca.33696.

49. Yokogami, K., Wakisaka, S., Avruch, J., and Reeves, S.A. (2000). Serine phosphorylation and maximal activation of STAT3 during CNTF signaling is mediated by the rapamycin target mTOR. Curr. Biol. *10*, 47–50. https://doi.org/10.1016/s0960-9822(99)00268-7.

50. Benight, N.M., and Waltz, S.E. (2012). Ron receptor tyrosine kinase signaling as a therapeutic target. Expert Opin. Ther. Targets *16*, 921–931. https://doi.org/10.1517/14728222.2012.710200.

51. Wan, X., Zhou, M., Huang, F., Zhao, N., Chen, X., Wu, Y., Zhu, W., Ni, Z., Jin, F., Wang, Y., et al. (2021). AKT1-CREB stimulation of PDGFRalpha expression is pivotal for PTEN deficient tumor development. Cell Death Dis. *12*, 172. https://doi.org/10.1038/s41419-021-03433-0.

52. Li, C., Lee, P.S., Sun, Y., Gu, X., Zhang, E., Guo, Y., Wu, C.L., Auricchio, N., Priolo, C., Li, J., et al. (2014). Estradiol and mTORC2 cooperate to enhance prostaglandin biosynthesis and tumorigenesis in TSC2-deficient LAM cells. J. Exp. Med. *211*, 15–28. https://doi.org/10.1084/jem.20131080.

53. Yu, G., Wang, L.G., Han, Y., and He, Q.Y. (2012). clusterProfiler: an R package for comparing biological themes among gene clusters. OMICS *16*, 284–287. https://doi.org/10.1089/omi.2011.0118.

54. Tang, Z., Li, C., Kang, B., Gao, G., Li, C., and Zhang, Z. (2017). GEPIA: a web server for cancer and normal gene expression profiling and interactive analyses. Nucleic Acids Res. *45*, W98–W102. https://doi.org/10.1093/nar/gkx247.